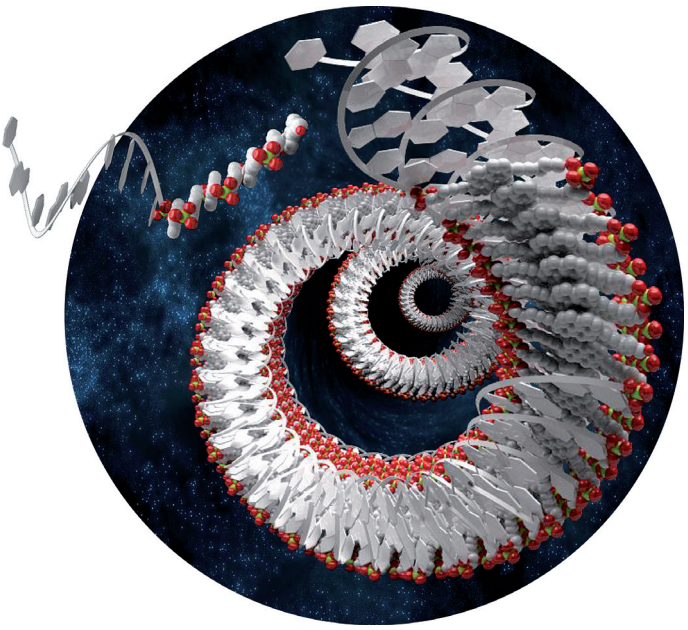

… combine the intrinsic properties of self-assembled materials with the potential of sequence-specific functionalization. In their Communication on page 7934 ff., R. Häner and co-workers describe the supramolecular polymerization of chimeric pyrene–DNA oligomers. The formation of helical ribbon structures is driven by pyrene stacking interactions and enables the controlled arrangement of oligonucleotide strands along the edges of the supramolecular polymers.

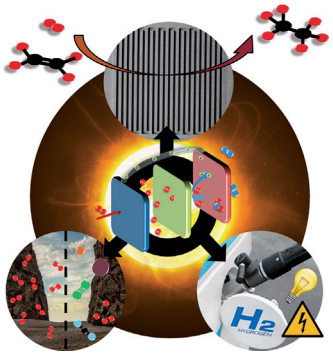

Hydrogen Separation

A short-circuited fuel cell with a Nafion membrane is used by J. Caro et al. in their Communication on page 7790 ff., to separate hydrogen from exhaust gases.

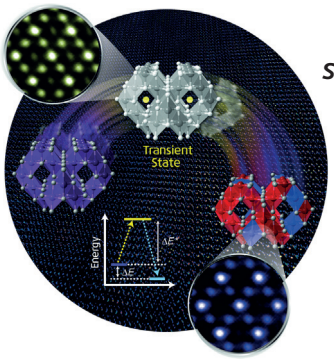

Solid-State Structures

In their Communication on page 7963 ff., S.-Y. Chung et al. report the configurational ordering in an AB_2O_4 spinel by the formation of Frenkel defects at octahedral sites as a transient state.

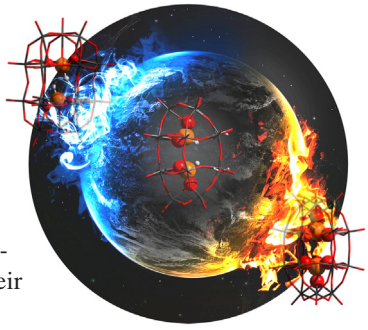

Polyoxometalate Clusters

A Dawson-like polyoxometalate cluster, $[W_{18}O_{56}(HP^{III}O_3)_2(H_2O)_2]^{8-}$, with a redox-active core which undergoes structural rearrangement in solution is reported by, L. Cronin et al. in their Communication on page 7895 ff.

How to contact us:

Editorial Office:
E-mail: angewandte@wiley-vch.de
Fax: (+49) 62 01–606-331
Telephone: (+49) 62 01–606-315

Reprints, E-Prints, Posters, Calendars:
Carmen Leitner
E-mail: chem-reprints@wiley-vch.de
Fax: (+49) 62 01–606-331
Telephone: (+49) 62 01–606-327

Copyright Permission:
Bettina Loycke
E-mail: rights-and-licences@wiley-vch.de
Fax: (+49) 62 01–606-332
Telephone: (+49) 62 01–606-280

Online Open:
Margitta Schmitt, Carmen Leitner
E-mail: angewandte@wiley-vch.de
Fax: (+49) 62 01–606-331
Telephone: (+49) 62 01–606-315

Subscriptions:
www.wileycustomerhelp.com
Fax: (+49) 62 01–606-184
Telephone: 0800 1800536 (Germany only)
+44(0) 1865476721 (all other countries)

Advertising:
Marion Schulz
E-mail: mschulz@wiley-vch.de
jspiess@wiley-vch.de
Fax: (+49) 62 01–606-550
Telephone: (+49) 62 01–606-565

Courier Services:
Boschstrasse 12, 69469 Weinheim

Regular Mail:
Postfach 101161, 69451 Weinheim

Angewandte Chemie International Edition is a journal of the Gesellschaft Deutscher Chemiker (GDCh), the largest chemistry-related scientific society in continental Europe. Information on the various activities and services of the GDCh, for example, cheaper subscription to *Angewandte Chemie International Edition*, as well as applications for membership can be found at **www.gdch.de** or can be requested from GDCh, Postfach 900440, D-60444 Frankfurt am Main, Germany.

GDCh
Gesellschaft Deutscher Chemiker

Service

Author Profile

"If I had one year of paid leave I would sail around the world with my family. If I could be a piece of lab equipment, I would be a magnetic stirrer, simple but essential …"
This and more about Yusuke Yamauchi can be found on page 7742.

News

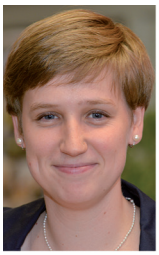
S. Riniker

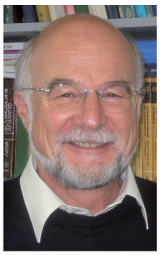
C. Bräuchle


H.-J. Freund


S. W. Hell


F. Diederich

Obituaries

Robert (Bob) J. P. Williams, one of founding fathers of bioinorganic chemistry, died on the 21st March 2015. His studies on the roles of metal ions in biological systems brought unprecedented insights into the structure, function, and dynamics of metalloproteins; this led to a better understanding of biological signaling, electron-transfer processes, and enzyme catalysis.

Books

Nobel Lectures

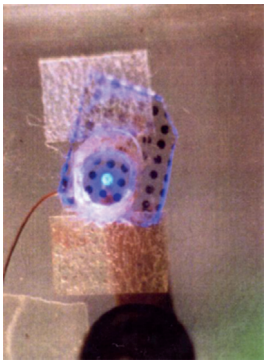

In the beginning there was light: Mankind has pursued light sources since ancient times, starting with flames, then the development of electric light bulbs much later, and most recently the production of light-emitting diodes. Isami Akasaki describes the historical progress that led to the invention of the first blue LED and related optical devices.

Growing success: The invention of a method to grow gallium nitride (GaN) on sapphire substrate formed the basis for the development of flat screens and smart displays based on blue-light-emitting diodes. Hiroshi Amano gives a personal account of the background of the studies that led to the technologies for growing GaN and producing p-GaN.

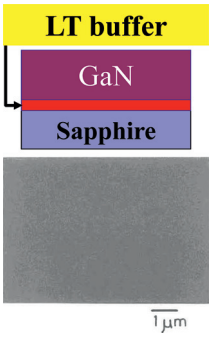

In the 1980s, all known material systems possessing the necessary properties for blue-light emission had shortcomings, thus negating their utilization in efficient LEDs. Gallium nitride (GaN) was one possible candidate, though, at the time, no *p*-type or active layer could be created. These challenges were ultimately overcome by Shuji Nakamura, who describes the path to the first blue GaN LED in his Nobel Lecture.

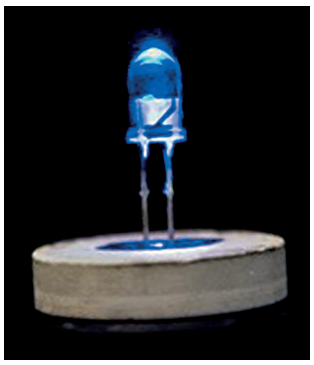

For the USA and Canada:
ANGEWANDTE CHEMIE International Edition (ISSN 1433-7851) is published weekly by Wiley-VCH, PO Box 191161, 69451 Weinheim, Germany. US mailing agent: SPP, PO Box 437, Emigsville, PA 17318. Periodicals postage paid at Emigsville, PA. US POSTMASTER: send address changes to *Angewandte Chemie*, John Wiley & Sons Inc., C/O The Sheridan Press, PO Box 465, Hanover, PA 17331. Annual subscription price for institutions: US$ 11.738/10.206 (valid for print and electronic / print or electronic delivery); for individuals who are personal members of a national chemical society prices are available on request. Postage and handling charges included. All prices are subject to local VAT/sales tax.

Communications

Fuel cell turned on its head: A short-circuited PEM fuel cell with a Nafion membrane can separate hydrogen from exhaust gases of different compositions at room temperature. The permeated hydrogen can either be obtained using an inert flushing gas or used directly in catalytic hydrogenations or combustion processes with reactive flushing gases.

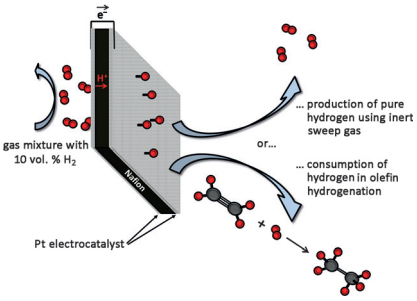

Hydrogen Separation

Frontispiece

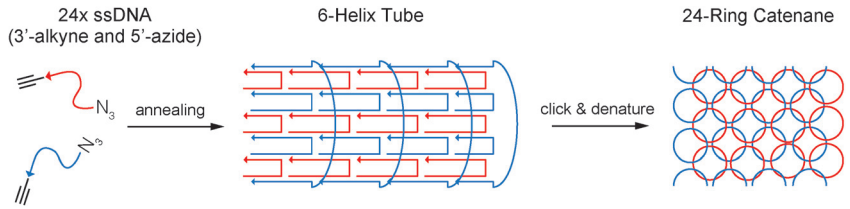

DNA Nanostructures

Interlocked catenane rings consisting of 24 single-stranded DNA molecules ("chain-armor DNA") were built from six helix tubes containing 3′-alkyne- and 5′-azide-modified single-stranded tiles (SST) that were covalently closed by click chemistry. Intramolecular cyclization stabilized these DNA nanotubes efficiently against enzymatic and thermal degradation.

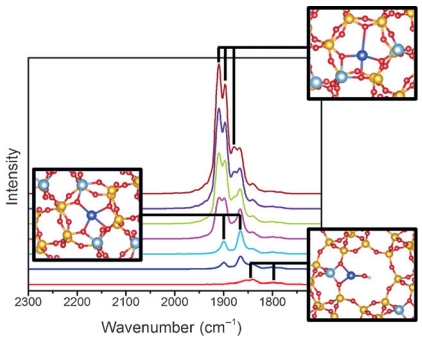

Theory and practice: The IR spectra of NO adsorbed on Cu centers in a copper-containing zeolite were modeled using molecular dynamics simulations. The spectra are complex, which is due to the thermal motions of the cations and the adsorbates, and are in excellent agreement with the experimental spectra.

Zeolite Structures

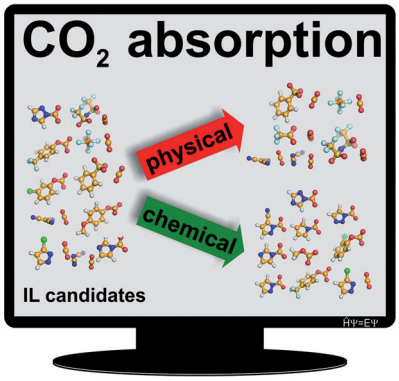

Better by design: Using a continuum model makes it possible to distinguish between the chemical and physical absorption of CO_2 in ionic liquids. The ionic liquids showing chemical adsorption were further narrowed down to "good" candidates, in which a facile desorption is feasible according to a calculated energy criterion. This criterion was determined by correlating the calculated Gibbs free energies with experimental capacities.

CO_2 Absorption

Proteasome Inhibitors

Every little counts: Proteasome inhibitors are potent drugs for cancers. X-ray analysis and activity assays revealed that nonpeptide belactosine derivatives target the S1 and primed sites of β5 subunits with high affinity. These β-lactones are less cytotoxic than currently applied proteasome inhibitors and analogues varying only in one methyl group show a six-fold difference in their affinity for the immunoproteasome.

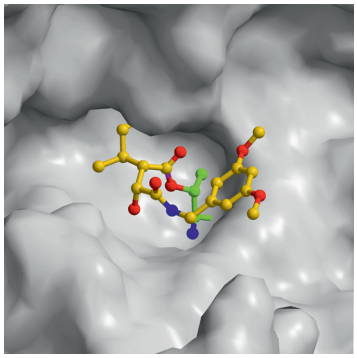

Breath Analysis

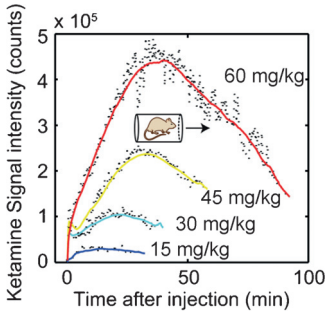

A noninvasive in vivo method based on secondary electrospray ionization mass spectrometry was used to determine the pharmacokinetics of drugs and their metabolites from the breath of a single mouse in real time. As an example, the pharmacokinetics of the antidepressant and anaesthetic drug ketamine and its metabolites was studied with a time resolution of 10 s per data point.

Boron-Nitrogen Heterocycles

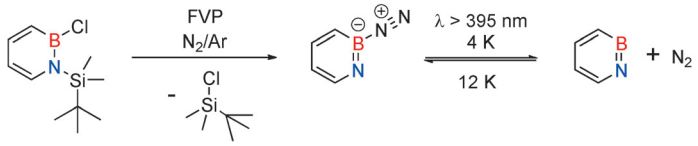

Azaborine in a flash: The boron–nitrogen derivative of *ortho*-benzyne, 1,2-azaborine, can be synthesized by flash vacuum pyrolysis (FVP) and trapped under cryogenic conditions to form a Lewis acid/base complex with nitrogen. Irradiation generates the free 1,2-azaborine which readily reacts with dinitrogen at slightly elevated temperatures.

Diels–Alder Reactions

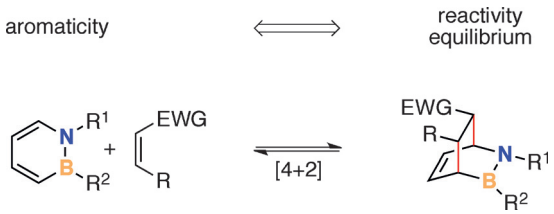

BN in control: The first [4+2] cycloaddition reaction of the 1,2-azaborine heterocycle is described. Both the N and the B substituent of the 1,2-azaborine exert significant influence on the aromaticity of the heterocycle and consequently the [4+2] cycloaddition reactivity. EWG = electron withdrawing group.

Antimony Complexes

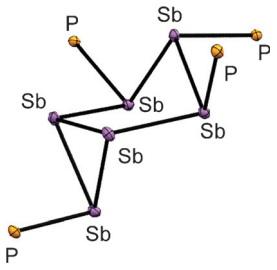

Grab a chair: A reductive catenation method has been used to prepare the first bicyclic *catena*-antimony cation $[(Ph_3P)_4Sb_6]^{4+}$. Formed by an unprecedented 14-electron redox process, the cation features a bicyclo[3.1.0]hexastibine core (see picture) stabilized by four phosphine ligands.

Radical Anions

The radical anion of octa-*tert*-butyloctasilacubane was generated and isolated (see picture). The X-ray crystallographic analysis showed that the Si–Si bonds are shortened and the Si–C bonds are elongated compared with those of octa-*tert*-butyloctasilacubane. These results are well explained by the distribution of an unpaired electron in the singly occupied molecular orbital (SOMO).

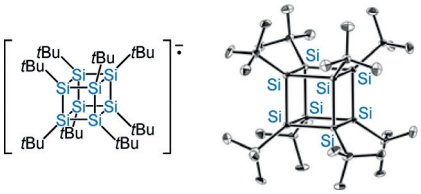

Synthetic Methods

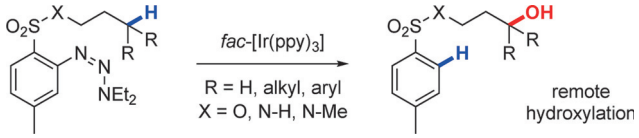

Mild conditions have been developed for the remote functionalization of aliphatic C–H bonds through radical translocation and oxidation of the resulting radical to the carbocation as a prerequisite to nucleophilic attack. The employment of *fac*-[Ir(ppy)$_3$] together with the Tz^o group facilitates the site-selective replacement of inert C–H bonds with a C–OH group.

Natural Products

Moving methyl groups: Hajos–Parrish ketone isomers with a transposed methyl group, termed "iso-Hajos–Parrish ketones", are useful building blocks for diverse targets. A new synthetic method to cyclopentenones is used in a three-step approach to several of these compounds. Furthermore, a natural product that was previously accessed in 18 steps was now synthesized in 10 steps using an iso-Hajos–Parrish ketone.

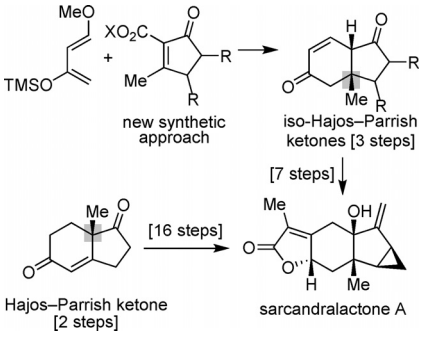

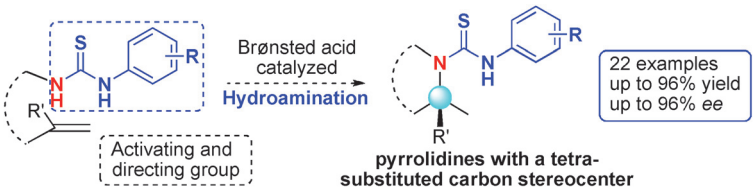

The enantioselective Brønsted acid catalyzed intramolecular hydroamination of alkenes is enabled by the use of a thiourea group that acts as both the activating and directing group by cooperative multiple hydrogen bonding. This method can be employed for the efficient construction of a series of chiral (spirocyclic) pyrrolidines and tricyclic amines with α-tetrasubstituted carbon stereocenters.

Organocatalysis

Planting the right seeds: Combining dynamic covalent chemistry with seeded self-assembly allows access to self-synthesizing fibers and block co-fibers with excellent control over length and polydispersity (PDI). Kinetically controlled assembly of self-synthesizing peptide-functionalized macrocycles occurs through a nucleation and growth mechanism when a seed is present.

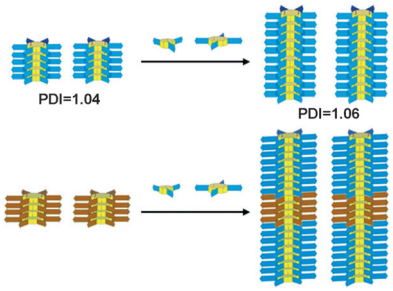

Systems Chemistry

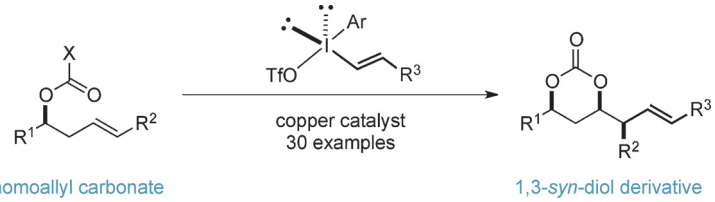

Polyols: The reported copper-catalyzed oxy-alkenylation strategy works well for a range of readily available, substituted homoallylic alcohol derivatives and alkenyl(aryl) iodonium salts to form *syn*-1,3-carbonates in excellent yield and high selectivity. Furthermore, the products formed are amenable to an iterative reaction sequence, thus affording highly complex polyketide-like fragments.

Synthetic Methods

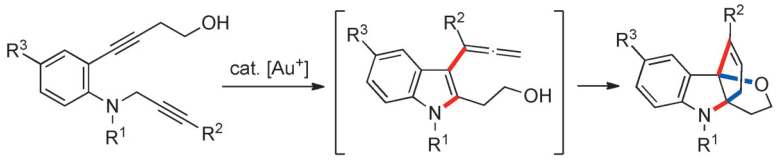

Heart of gold: A rapid access to fused three-dimensional indolines has been developed in which four bonds and three rings are formed in a single operation. Under gold catalysis, a propargyl substituent migrates from an aniline nitrogen atom to the C3-position of an indole from 2-alkynyl-*N*-propargylanilines to give the tetracyclic fused indolines directly (see scheme).

Homogeneous Gold Catalysis

Borylation

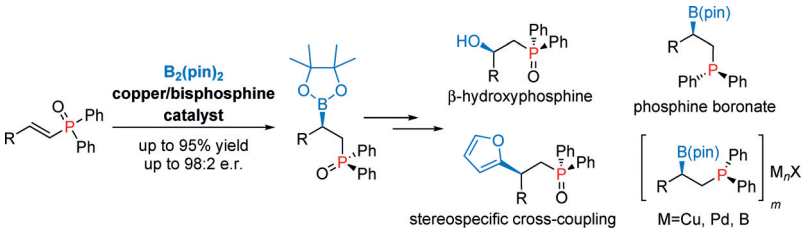

Ambiphilic phosphine boronate esters are obtained by the asymmetric boration of α,β-unsaturated phosphine oxides with a copper/bisphosphine catalyst in good yields and high enantioselectivity. The synthetic utility of the products is demonstrated through stereospecific transformations into multifunctional optically active compounds.

Inside Cover

Hypervalent Iodine

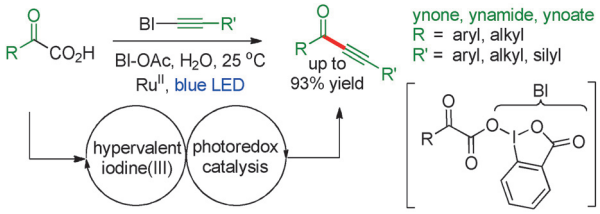

Cool cats: Ynones, ynamides, and ynoates have been constructed at room temperature from substrates with various sensitive and reactive functional groups by using a combination of hypervalent iodine(III) reagents (HIRs) and photoredox catalysis with visible light. The reaction proceeds by formation of an acyl radical from α-ketoacids followed by an unprecedented acyl radical addition to HIR-bound alkynes.

Photoelectrochemical Cells

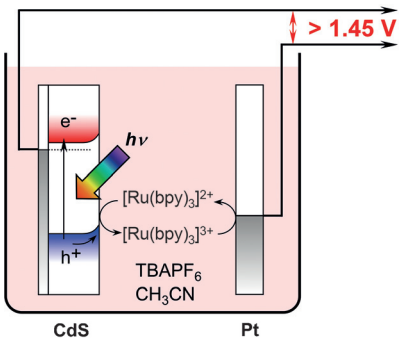

A CdS photoanode and Pt counter electrode as a photoelectrochemical cell with the redox shuttle of the ruthenium–2,2′-bipyridine complex $[Ru(bpy)_3]^{2+/3+}$ in a non-aqueous electrolyte was studied. An open-circuit voltage of 1.48 V, short-circuit current of 3.88 mA cm^{-2}, and fill factor of 0.49 were obtained. TBA = tetra-*n*-butylammonium.

Cluster Compounds

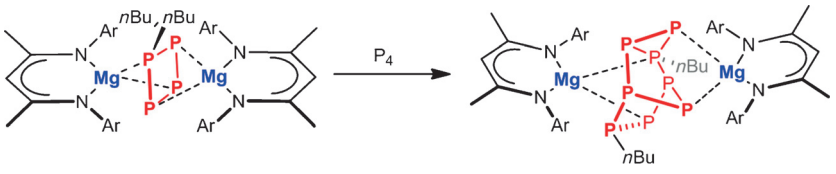

Taking the P: The controlled, sequential activation of white phosphorus (P_4) can be mediated by organomagnesium compounds with appropriate supporting ligands. The activation leads to the highly discriminating synthesis of unusual $[nBu_2P_4]^{2-}$ and $[nBu_2P_8]^{2-}$ cluster dianions.

In^{3+} befriending Cr^{3+}: Indium and chromium ions drag each other into unprecedented heterometallic In-Cr-MOP (metal–organic polyhedra) crystals. These have a high proton conductivity (5.8×10^{-2} S cm^{-1}) at 22.5 °C and 98% relative humidity for a single crystal.

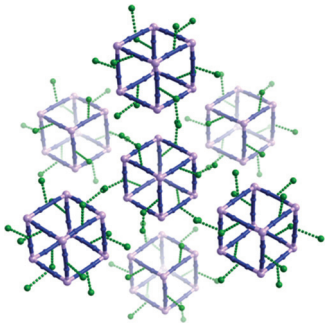

Metal–Organic Polyhedra

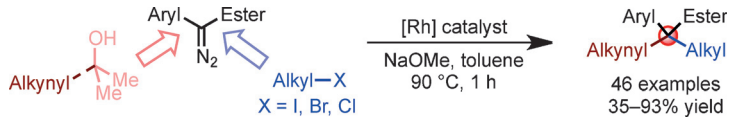

All on C: A sequential Rh^{I}-catalyzed alkyl and alkynyl coupling on a carbene successively establishes a C(sp)–C(sp^3) and then a C(sp^3)–C(sp^3) bond on the original carbenic carbon center. The reaction results in the formation of an all-carbon quaternary center in high efficiency. A rhodium–carbene migratory insertion is proposed as the key step in this transformation.

Carbenes

Caught in a trap: A tungsten-based Dawson-like polyoxometalate cluster $[W_{18}O_{56}(HP^{III}O_3)_2(H_2O)_2]^{8-}$ has been isolated. NMR spectroscopy and ESI-MS show that in solution, the cluster undergoes a structural rearrangement whereby the {HPO_3} moieties dimerize through interphosphite interactions. In the solid state, the cluster underwent a temperature-dependent intramolecular redox reaction ($P^{III} \rightarrow P^{V}$). Atom colors: W = gray; O = red; P = orange; H = light gray.

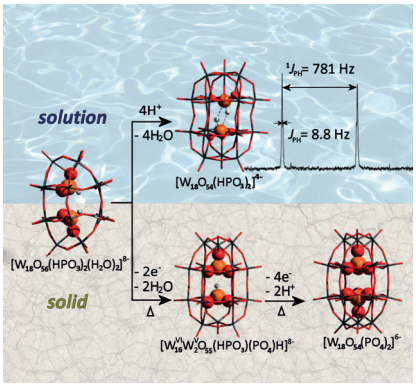

Polyoxometalates

A simple yet multifaceted magnesium monocarborane (MMC) based electrolyte was prepared. This remarkable halogen-free and benign system is compatible with Mg metal and displays the highest anodic stability reported to date. The non-corrosive nature of the MMC electrolyte enabled the examination of high-voltage cathodes in a coin cell, which is a critical step forward in realizing practical rechargeable Mg batteries.

Magnesium Batteries

Perovskite Solar Cells

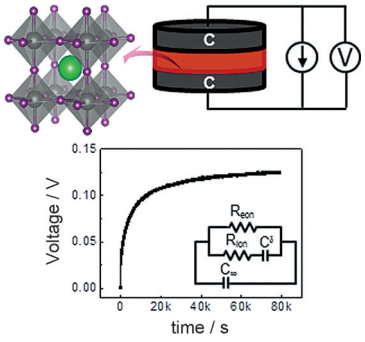

In alkyl ammonium iodide ion conduction turns out to be substantial. The resulting stoichiometric polarization can explain anomalous features in perovskite solar cells: huge apparent low-frequency permittivity and hysteretic current–voltage behavior in cyclic sweep experiments.

Metabolic Labeling

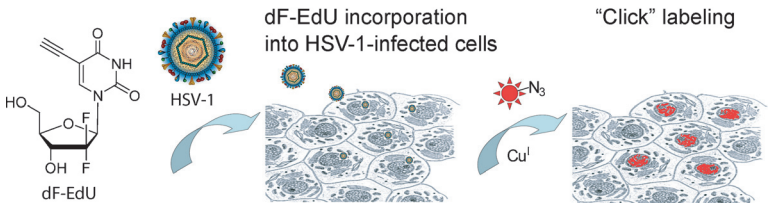

Pathogen-induced metabolic labeling: Cells infected by Herpes Simplex Virus-1 (HSV-1) were selectively labeled with the gemcitabine metabolite analogue dF-EdU and an azide-conjugated fluorophore. Labeling selectivity is due to the phosphorylation of dF-EdU by viral but not human thymidine kinases. These results establish a new approach for pathogen-specific bioorthogonal chemical labeling.

Rattle-Structured Nanoprobe

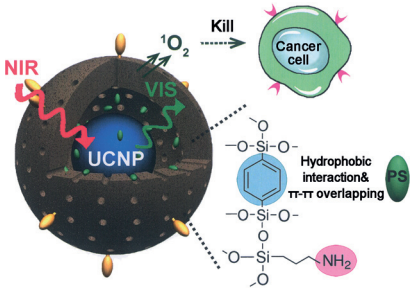

Rattle-structured nano-bioprobes featuring a β-$NaLuF_4$:Gd/Yb/Er core and a benzene-bridged organosilica shell exhibit a high loading capacity and the disaggregation effect of photosensitizers, providing enhanced photodynamic therapy. Together with the functions of upconversion/X-ray computed tomography (UC/CT) dual-modal imaging and tumor-targeting, these nanoprobes are highly promising for cancer theranostics.

Synthetic Methods

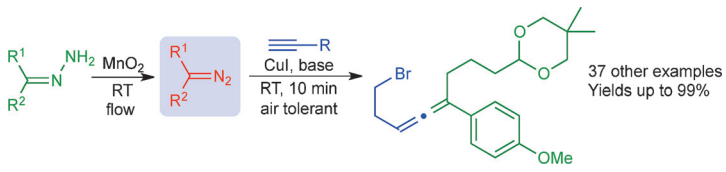

Well tolerated: A mild copper-catalyzed coupling reaction between unstabilized diazo compounds (generated in flow) and terminal alkynes is reported. The method provides di- and trisubstituted allenes with high functional-group tolerance.

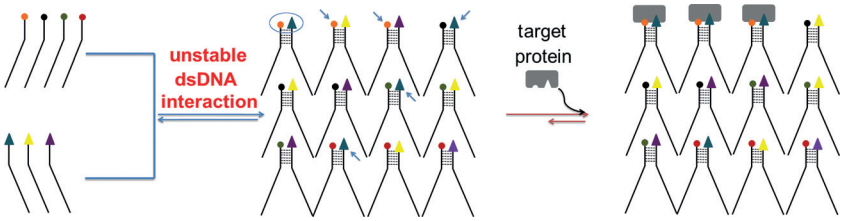

Selection goes dynamic: Dynamic combinatorial chemistry explores the thermodynamic equilibrium of reversible reactions. DNA-encoded chemical libraries enable the selection of binders from compound mixtures. Now the advantages of DNA-encoded dynamic combinatorial chemical libraries for the selection of protein binders from a myriad of compounds (see picture) and for DNA-templated reactions are demonstrated.

Drug Discovery

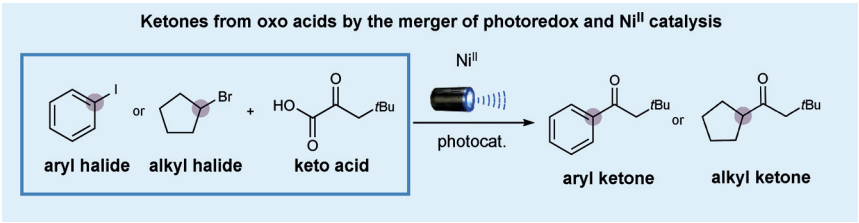

The direct decarboxylative arylation of α-oxo acids has been achieved by synergistic visible-light-mediated photoredox and nickel catalysis. This method offers rapid entry to aryl and alkyl ketone architectures from simple α-oxo acid precursors via an acyl radical intermediate. Significant substrate scope is observed with respect to both the oxo acid and arene coupling partners.

Dual Catalysis

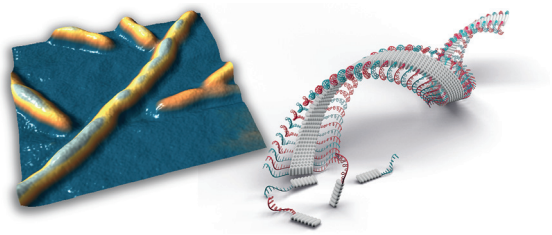

Ribboned: Short chimeric DNA–pyrene oligomers were used as precursors for the formation of DNA-grafted supramolecular polymers. Within these polymers, the oligodeoxynucleotide strands are arranged along the edges of a ribbon-shaped helical aggregate of self-assembled pyrene segments.

DNA Nanotechnology

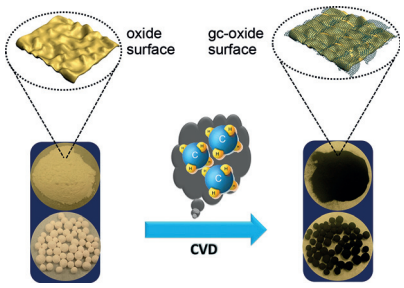

Protected catalyst support: Depositing graphitic carbon onto oxides can effectively protect the oxide surface from attack by water under harsh conditions. The graphitic carbon/oxide composite supported catalysts exhibit excellent stability (even under acidic conditions) for biomass conversion reactions. CVD = chemical vapor deposition.

Heterogeneous Catalysis

Supramolecular Hydrogels

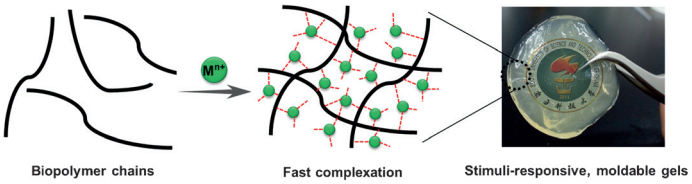

Turning to jelly: A series of metal–biopolymer hydrogels is obtained by ultrafast supramolecular complexation. The hydrogels are easily prepared, have high water content, and are stable at room temperature. The multistimuli-responsive Ag-based hydrogel can be molded to form shape-persistent, free-standing objects.

Platinum Complexes

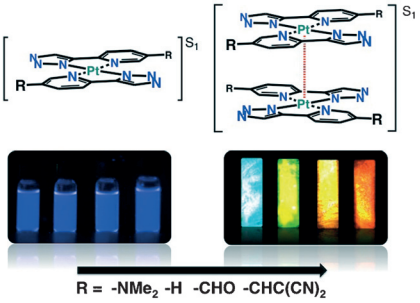

Turn-on tunability: A series of bis-4-(2-pyridyl)-1,2,3-triazolatoplatinum(II) complexes display variable emission tunability. At low concentration, the emission can be tuned only slightly by changing the nature of the substituent but at higher concentrations tunability is enhanced. This "turn-on" sensitivity in the excimeric emission is attributed to strong Pt–Pt metallophilic interactions and a change in the excited-state character.

DOI: 10.1002/anie.201582714

Flashback: 50 Years Ago . . .

Hetarynes (*o*-didehydroaromatic compounds with heteroatoms in the ring) were the topic of a Review by T. Kauffmann, who discussed the synthesis and properties of these compounds. In another Review article, K.-D. Gundermann outlined recent progress in the chemiluminescence of organic compounds, which was made easier by the development of sensitive equipment. Luminol firefly luciferin, and lucigenin were among the compounds discussed.

E. G. Rochow and P. Geymayer reported on the synthesis of *N*,*N*′-bis(chlorodimethylsilyl)tetramethylcyclodisilazane, which was produced by the reaction of 1,3-dichlorotetramethyldisilazane with sodium bistrimethylsilylamide. The product was regarded as a potential starting material for polymer synthesis.

G. Köbrich and H. Heinemann published a Communication on tri(isopropylidene)cyclopropane. The analogous trimethylenecyclopropane was predicted to polymerize in the solid state, however, the hexamethyl derivative could be prepared from the reaction of tetramethylbutatriene with α-bromo-β,β-dimethylvinyllithium and was found to be extremely stable.

H.-P. Boehm et al. reported on the reaction of organolithium compounds with silicon dioxide upon heating the reactants in ether for around 8 hours. A range of products were formed from phenyllithium, including tetraphenylsilane, triphenylsilanol, and diphenylsilandiol; the reaction was thought to occur by a nucleophilic attack on surface siloxane bonds. Boehm was one of the first to report the synthesis and characterization of graphene films (for his personal account see *Angew. Chem. Int. Ed.* **2010**, *49*, 9332).

Read more in Issue 7/1965.

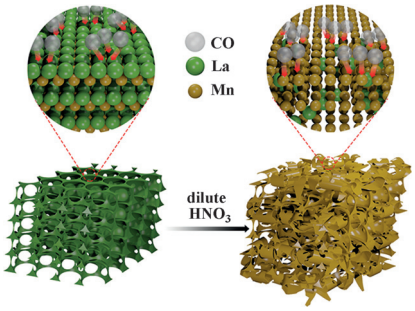

Remove to improve: A novel γ-MnO_2-like catalyst was prepared by selective dissolution of La with dilute HNO_3 in $LaMnO_3$ perovskite. Upon the removal of La, the obtained material possessed a large surface area and improved surface oxygen species, resulting in a significant higher catalytic activity on CO oxidation (T_{50} = 89 °C) than the initial precursor $LaMnO_3$ (T_{50} = 237 °C) and ordinary γ-MnO_2 (T_{50} = 148 °C).

Perovskite Phases

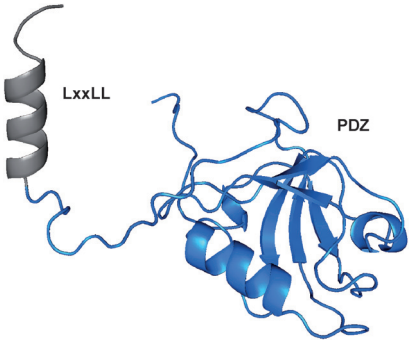

Double duty: A bifunctional inhibitory ligand of human papillomaviruses (HPV) E6 oncoproteins was developed by combining the minimal E6-binding regions of two key cellular targets of E6: a PDZ domain from the polarity protein MAGI1, and an LxxLL motif from the ubiquitin ligase E6AP. The PDZ-LxxLL chimera binds high-risk mucosal HPV E6 proteins with nanomolar affinity and induces apoptotic death in HPV-positive cells derived from cervical tumors.

Peptide Therapeutics

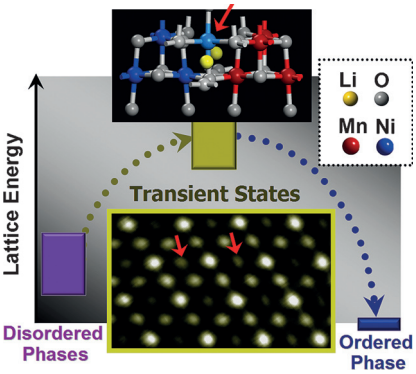

Defective mediators: *B*-site configurational ordering in an AB_2O_4-type spinel oxide takes place by the formation of Frenkel-type defects which form the crucial transient state. A precise suggestion of the transient states (see picture) and the resulting kinetic pathway during the ordering transition is provided.

Solid-State Structures

Inside Back Cover

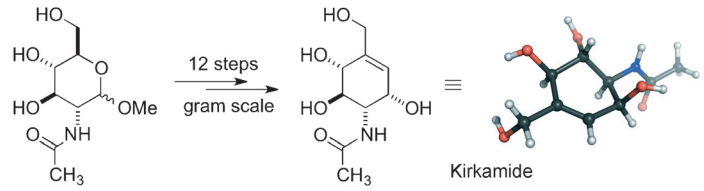

Better together: The chemical nature of the interaction between the plant *Psychotria kirkii* and its bacterial symbiont remains unclear. Genomic analysis of the microorganism, which forms nodules under the leaves of the host, suggested the presence of a C_7N aminocyclitol. Following isolation, structure elucidation, and total synthesis, this compound, termed kirkamide, was shown to be toxic to insects and aquatic arthropods.

Natural Products

Light–Matter States

Good vibrations: Ground-state molecular vibrations can be hybridized through strong coupling with the vacuum field of a cavity optical mode in the infrared region, leading to the formation of two new coherent vibro-polariton states. Raman scattering cross-section from the hybridized light–matter states can be boosted by two to three orders of magnitude as a result of strong coupling.

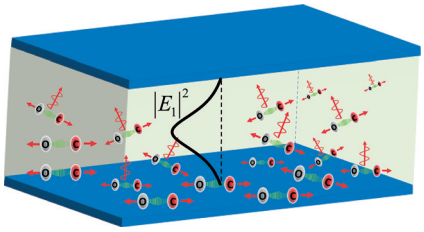

Crystallization

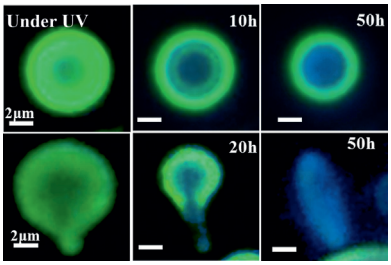

Crystallization of microparticles can be observed in situ and in real time by fluorescence microscopy by utilizing a novel organic chromophore with morphology-dependent fluorescence. Perfectly spherical microparticles nucleate at the interior and growth is confined to the inner part, ending with a core–shell structure (see picture, top). Defects of the surface prior to crystallization can lead to a complete crystal (bottom).

Homogeneous Catalysis

Lucky pendant: Ce^{4+}-driven water oxidation catalyzed by a mononuclear ruthenium complex was observed to be accelerated following the introduction of pendant SO_3^- groups to the catalyst, which are able to capture Ce^{4+} ions. The results of this work indicate that modification of the secondary coordination sphere is an effective strategy for the development of catalysts for water oxidation.

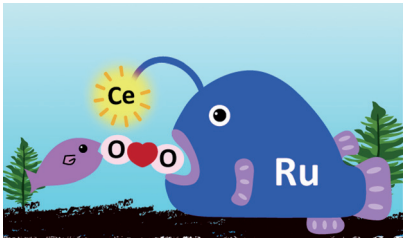

Fluorescence Memory

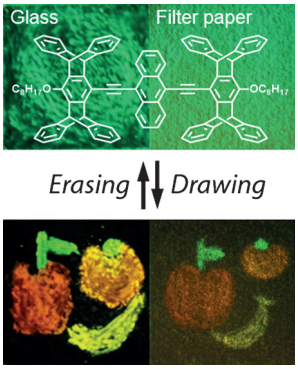

Memorable art: Multicolor fluorescence writing was possible on thin solid films of a pentiptycene–anthracene conjugated system (see picture). This technique relies on the formation of fluorescent exciplexes with aniline vapors and on force-induced fluorescence color memory. The drawings were erased by blowing air over the surface and by exposure to dichloromethane fumes.

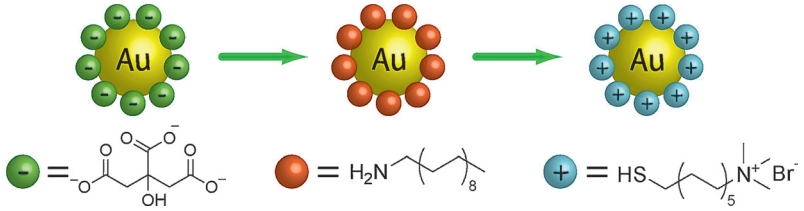

Be positive! Cationic gold nanoparticles with tunable sizes from 8 to 20 nm can be prepared by a rapid and scalable two-step phase-transfer protocol that starts from simple citrate-capped particles and proceeds via neutral octadecylamine-capped nanoparticles (see figure). The cationic gold nanoparticles form ordered self-assembled structures with negatively charged biological components through electrostatic interactions.

Nanostructures

Crystallized film: A novel organic–inorganic hybrid nanoporous material with alternately laminated lipophilic and hydrophilic nanospaces was synthesized. It shows microporous adsorption for both hydrophilic and lipophilic adsorptives, and its outer surface tightly adsorbs lysozyme.

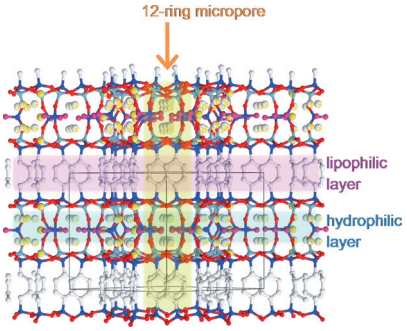

Organic–Inorganic Hybrids

Supporting information is available on www.angewandte.org (see article for access details).

A video clip is available as Supporting Information on www.angewandte.org (see article for access details).

This article is available online free of charge (Open Access).

This article is accompanied by a cover picture (front or back cover, and inside or outside).

The Very Important Papers, marked VIP, have been rated unanimously as very important by the referees.

The Hot Papers are articles that the Editors have chosen on the basis of the referee reports to be of particular importance for an intensely studied area of research.

Check out these journals:

www.chemasianj.org

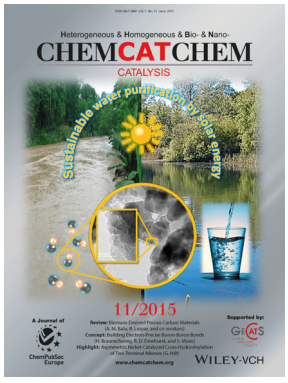

www.chemcatchem.org

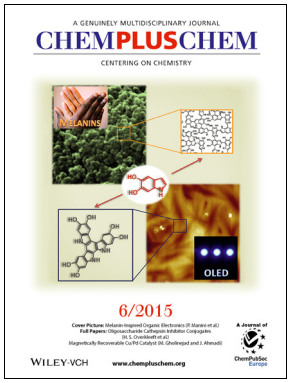

www.chempluschem.org

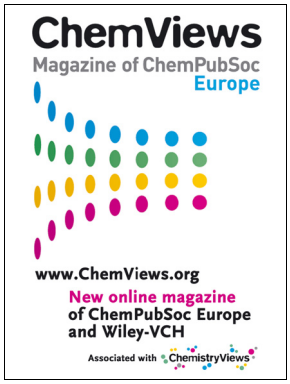

www.chemviews.org

Angewandte Corrigendum

Conformation-Specific Circular Dichroism Spectroscopy of Cold, Isolated Chiral Molecules

A. Hong, C. M. Choi, H. J. Eun, C. Jeong, J. Heo,* N. J. Kim* ——— **7805–7808**

Angew. Chem. Int. Ed. **2014**, *53*

DOI: 10.1002/anie.201403916

In this Communication, the plus and minus signs of the circular dichroism (CD) spectra in Figures 2b and 4b were incorrect. The corrected Figures are shown below. Additionally, after further theoretical investigation, it was found that the signs of the rotatory strengths (*R*) for pseudoephedrine (pED) vary depending on the type of the density functionals used in the time-dependent density functional theory (TDDFT) calculations. This variation is due to small CD effects of the S_0–S_1 transition of pED and large error bars of the CD values predicted by theory. Table S1 in the Supporting Information lists the *R* values estimated using various density functionals.

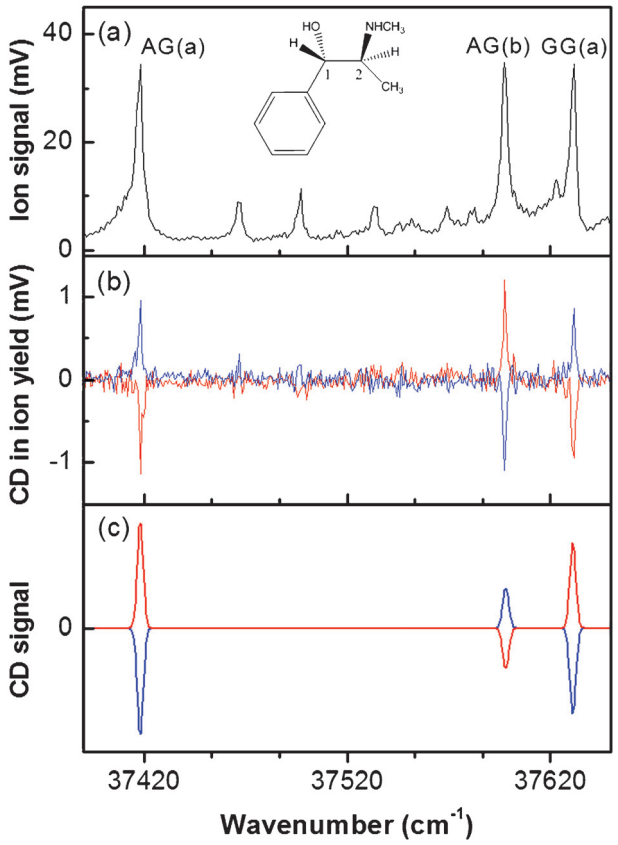

Figure 2. a) R2PI spectrum of *S*-pED near the origin band of the S_0–S_1 transition. The inset shows the structure of *S*-pED. The number of ions produced by a single-laser pulse at the origin bands was roughly estimated as about 900. b) R2PI CD spectra of *S*- (blue line) and *R*-pED (red line). The *g* values at the bands of AG(a), AG(b), and GG(a) of *S*-pED were measured as $+0.026 \pm 0.005$, -0.025 ± 0.006, and $+0.024 \pm 0.005$, respectively. c) Theoretical CD spectra of *S*- (blue line) and *R*-pED (red line) obtained with the rotatory strength, *R*, calculated using TDDFT at the M06-2X/6-311++G(d,p) level.

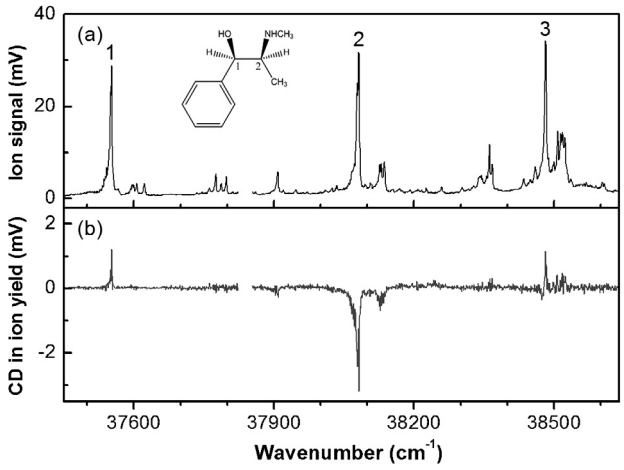

Figure 4. a) R2PI spectrum of *R*-ED near the origin band of the S_0–S_1 transition. The inset shows the structure of *R*-ED. The discontinuous region between 37825 and 37855 cm^{-1} is where the grating order of the dye laser changes. b) R2PI CD spectrum of *R*-ED. The *g* values of 1–3 bands were measured as $+0.030 \pm 0.011$, -0.091 ± 0.007, and $+0.041 \pm 0.013$, respectively.